INTEGRATED STRUCTURE-CONTROL DESIGN OPTIMIZATION OF AN UNMANNED QUADROTOR HELICOPTER (UGH) FOR OBJECT GRASPING AND MANIPULATION

Mohebbi, Abolfazl (1); Gallacher, Colin (2); Harrison, James (3); Willes, John (2); Achiche, Sofiane (1)
1: École Polytechnique de Montréal, Canada; 2: McGill University, Canada; 3: Stanford University, United States of America

Abstract

In this study, the problem of integrated system-level design optimization for a quadrotor equipped with a robotic arm and gripper is addressed and thoroughly discussed. First, the operational objectives and the mission of the system are defined and main components are introduced. Then the system level analysis is described in such a way that for the robotic gripper, manipulator and the quadrotor structure, a mechanical system-level optimization is formulated and in a bigger design integration loop, the overall mechanical-control system optimization is solved which guarantees an optimal system solution after a number of iterations. At the end, more detailed numerical results are discussed and analyzed.

Keywords: Mechatronics, Optimisation, Integrated product development, Control, Drones

Contact:
Abolfazl Mohebbi
École Polytechnique de Montréal
Mechanical Engineering
Canada
abolfazl.mohebbi@polymtl.ca

Please cite this paper as:
Surnames, Initials: *Title of paper*. In: Proceedings of the 21st International Conference on Engineering Design (ICED17), Vol. 4: Design Methods and Tools, Vancouver, Canada, 21.-25.08.2017.

1 INTRODUCTION

Quadrotors are highly agile aerial robots that have the ability to maneuver in both constrained and open environments. Recent advances in energy storage devices, sensors, actuators and information processing have bolstered the development of Unmanned Aerial Vehicle (UAV) platforms with diverse mission capabilities. One of the advantages of using a multi-rotor system over a traditional helicopter is to increase the payload capacity due to more lift. While the design of quadrotors is easily varied to suit mission requirements, design decisions are complicated by challenging interaction between subsystems (e.g. actuators, energy storage). Indeed, physical and operational constraints on the vehicle design, as well as the high degree of coupling between mechatronic subsystems, make the generation of a practical design that satisfies mission requirements a difficult task. Unmanned Quadrotor Helicopters (UQH) are excellent examples of highly coupled mechatronic systems where the disciplines of aerodynamics, structures and materials, flight mechanics and control are acting upon each other in a typical flight condition. In terms of system dynamics, a quadrotor is an under-actuated system with six DoF and four inputs which is inherently unstable and difficult to control (Bouabdallah and Siegwart, 2007).

The desire to tailor system design to specific mission requirements, subject to complex constraints, makes a multidisciplinary design optimization (MDO) approach appropriate. MDO has seen increasing use in commercial aircraft design in the previous two decades (Sobieszczanski-Sobieski and Haftka, 1997). However, most of the existing literature in quadrotor design optimization are focused on optimizing the flight control parameters (Chu and Duan, 2013; Yacef et al., 2013), a few other studies concentrated on design optimization of quadrotor structures and aerodynamics leaving out the control parameters. For example in a work by (Turkoglu et al., 2008), an automatic control system design for longitudinal flight dynamics based on Integral Squared Error (ISE) parameter optimization technique has been implemented on UAV dynamics. (Mohebbi et al., 2015) used the Design for Control (DFC) methodology for design of a complex mechatronic system. While the controller parameters were designed concurrently with structural parameters, the opportunity to improve the design using on-line change of controller parameters has been overlooked in this method. In this paper, an approach is proposed for system-level optimization of a quadrotor UAV that is capable of robotic manipulation. While it is assumed that an optimization effort has already been made for each sub-system, an integrated optimization loop is used to ensure system-level optimality. The rest of this paper is organized as follows: Section 2 states the design optimization problem. Section 3 recalls the quadrotor dynamic model while in Section 4, the mechanical system optimization is described. In Section 5, the integrated system-level optimization is conducted and the results are presented. Finally, the concluding remarks are discussed in Section 6.

2 DESIGN PROBLEM STATEMENT

Integrating the sensors, actuators and intelligence into a lightweight vertically flying system with a decent operation time is not trivial. The quadrotor is a complex multidisciplinary system with strong internal couplings which urge the use of an interdisciplinary approach. This is one reason why progress in advancing rotorcraft technology has been difficult (Hoffmann et al., 2007). The main goal of this paper is to achieve an optimal system-level design integration for a small quadrotor UAV capable of following a trajectory and finally, approaching and grasping a target with a robotic arm and gripper. This scenario is illustrated by Figure 1.

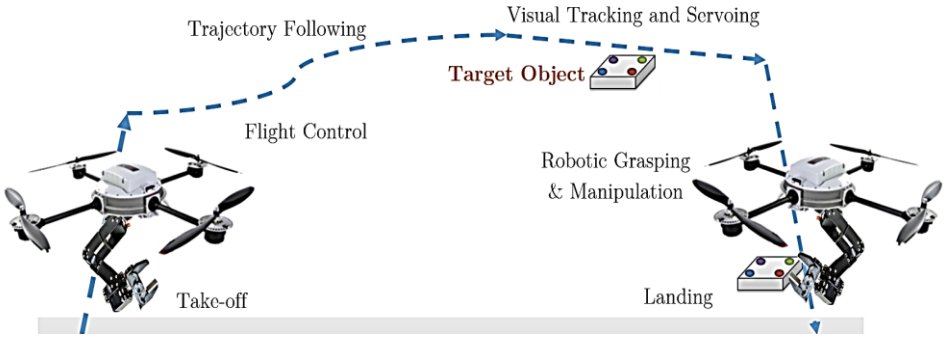

Figure 1. The mission to be carried out by the quadrotor system

The following four subsystems are chosen for further studies and optimization amongst all possible system components in a quadrotor system:

2.1 Frame and Structure

The ideal quadrotor is agile, powerful and capable of extended flight time, however, there are substantial trade-offs to consider in the design. A commonly encountered trade-off is the relationship between thrust and weight (e.g. more thrust can be achieved using more powerful motors, however, they require a more robust structure which increases the weight). The trade-offs are very difficult to heuristically optimize and the use of mathematical optimization allows for a deeper exploration. As outlined by (Magnussen et al., 2014), the quadrotor model to be optimized will be simplified using the following assumptions: The quadrotor is assumed to be planar with its origin to be the intersection of the rotor arms; the actuators are point masses located at the tip of the rotor arms; the battery is assumed to be a point mass located at the origin; the coefficients of thrust and power are assumed to be constant for all RPM. The objective function can be reduced to three optimizable components: 1) Payload Capacity, 2) Flight Time, and 3) Dynamic Performance. Each component will be weighted according to specific design considerations outlined in Section 4 and 5.

2.2 Robotic Serial Manipulator

The design of the 3R manipulator should allow for a large workspace with limited kinematic singularities. To reduce size and excess material, we aim to ensure the minimization of the size associated with the manipulator links. The performance of the manipulator itself is also very important for the tasks associated during pick and place operations. We use an index defined as the kinematic manipulability (Yoshikawa, 1985) that is associated with the ability to achieve large accelerations from small input torques.. Finally, the manipulator is intended to be attached to the main frame. The dynamics associated with the serial manipulator will impose forces on the structure. These forces must be countered by the quadrotor and so the manipulator dynamics will impact the stability. To account for this, the effective mass of the manipulator must be minimized which will reduce the inertial forces imparted to the quadrotor associated with rapid accelerations of the manipulator, and also improve flight time associated with a decrease in payload.

2.3 Gripper

The grasping and manipulation of an object by an aerial robot relies on a gripper that is lightweight and strong, with low power consumption. It is desirable to reduce device complexity while retaining grip strength and minimizing device weight. The model used in this paper is based on the Velo gripper (Ciocarlie et al., 2014), which consists of a two fingered gripper with one actuated degree of freedom. This gripper transfers passively between an enveloping grasp and a pinch, depending on the size and shape of the object. In this work, we aim at development of a gripper that is optimized versus constraints more directly relevant to the aerial manipulation tasks (e.g. linkage strength).

2.4 Control System

In order to enable the UQH to follow a predefined trajectory, a full control of attitude and position of the system is necessary. Accordingly, to control the attitude and altitude of the proposed quadrotor system, a PID controller is used. PID has shown good performance with low complexity and has already been investigated in many efforts (Salih et al., 2010; Szafranski and Czyba, 2011) to stabilize quadrotors. In this study, the structural properties are considered as input parameters from the structural design component. Thus, the main objective of this component design is to tune the PID gains by optimizing performance subjected to robustness, stability and other control requirements. Like every optimization problem, trade-offs are to be faced during the design of the PID controller.

3 SYSTEM MODELING AND DYNAMICS

In this paper, Euler-Lagrange formulation and DC motor equations are used to model the quadrotor system. It is assumed that the structure of the system is rigid and symmetric and the thrust and drag affecting the system are proportional to the squared speed of propellers. Figure 2 illustrates the coordinate system for the quadrotor model where □ is the world coordinate frame and B is the body fixed frame. Consequently, the quadrotor dynamic model describing the roll, pitch and yaw rotations contains of three terms which are the gyroscopic effect resulting from the rigid body rotation and from the propeller rotation coupled with the body rotation and finally the actuators action. Furthermore, the mechanical symmetry of the quadrotor allows one to consider the use of a diagonal inertia matrix. This model for roll-pitch-yaw motion is formulated as below:

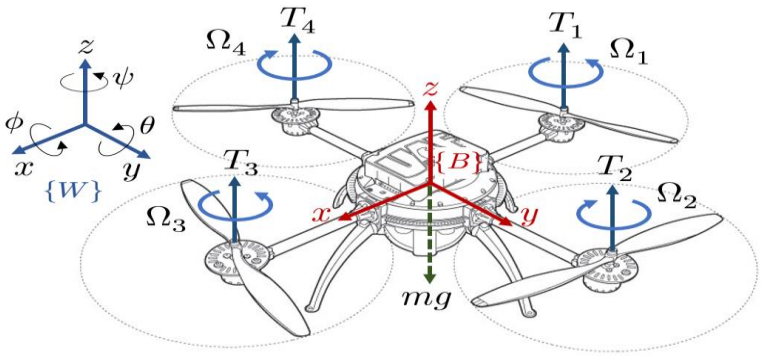

Figure 2. Quadrotor model coordinate system

$$\begin{cases} \ddot{\phi} = \frac{J_r\dot{\theta}(\Omega_1+\Omega_3-\Omega_2-\Omega_4)}{I_{xx}} + \frac{(I_{yy}-I_{zz})}{I_{xx}}\dot{\theta}\dot{\psi} + \frac{b_t l\,(\Omega_4^2-\Omega_2^2)}{I_{xx}} \\ \ddot{\theta} = \frac{J_r\dot{\theta}(\Omega_1+\Omega_3-\Omega_2-\Omega_4)}{I_{xx}} + \frac{(I_{yy}-I_{zz})}{I_{xx}}\dot{\theta}\dot{\psi} + \frac{b_t l\,(\Omega_4^2-\Omega_2^2)}{I_{xx}} \\ \ddot{\psi} = \frac{-d(\Omega_2^2+\Omega_4^2-\Omega_1^2-\Omega_3^2)}{I_{zz}} + \frac{(I_{xx}-I_{yy})}{I_{zz}}\dot{\phi}\dot{\theta} \end{cases} \quad (1)$$

where J_r is rotor inertia, Ω_i are propellers' speed, $[I_{xx}, I_{yy}, I_{zz}]$ are inertia moments and b_t is the propeller Thrust factor. Using a Newton dynamics formulation, we can also achieve the dynamics in translational coordinates as described in (Mohebbi et al., 2016). The rotors are considered to be driven by DC-motors with a low inductance. Thus, the second order DC-motor dynamics may be approximated by the following equation (Mohebbi et al., 2015):

$$\dot{w} = -Aw_m + Bu + C, \text{ where } A = \left(\frac{1}{\eta} + \frac{2dw_0}{\gamma r^3 J_t}\right), B = \left(\frac{1}{k_m \eta}\right), C = \left(\frac{dw_0^2}{\gamma r^3 J_t}\right), \eta = \frac{RJ_t}{k_m^2}. \quad (2)$$

in which u is the input voltage, w_m is motor's angular speed, γ and r are gearbox efficiency and reduction ratio respectively, k_m is the torque constant, d is propellers drag factor and J_t is the total rotor inertia.

4 MECHANICAL SYSTEM OPTIMIZATION

4.1 Problem Definition

A sub-system level analysis was completed for all components mentioned in Section 2. Each component was individually subjected to an optimization process to reach initial design goals. The quadrotor body was optimized to maximize the flight time with constraints on the payload capacity and the dynamic performance. The battery, propeller and motors were the three components chosen for optimization with the frame geometry being driven by the propeller size. The optimization of the elbow manipulator was a multi-objective problem to maximize the workspace volume, overall length, global kinematic and dynamic manipulability indices, while minimizing the total mass. Moreover, the gripper optimization problem was formulated as a weighted sum of two terms: the mass of the gripper and the number of graspable objects (as a fraction of the size of the Willow Garage Object Database (Garage, 2010)).

The results from sub-system level optimization are then fed into a bigger loop of mechanical system optimization. The mechanical system level optimization can be reduced to minimizing the inertia of the device. An analytical expression can be derived for the inertia displayed as a function of the design variables that make up the mechanical system. The quadrotor body inertia is given as follows:

$$I = diag(I_{xx}, I_{yy}, I_{zz}),\ I_{xx} = I_{yy} = 2a_{act}L_a^2 + \frac{2L_a^3\kappa}{3},\ I_{zz} = 2I_{xx} \quad (3)$$

Where, m_{act} is the motor and propeller mass, L_a is the rotor arm length and κ is the rotor arm mass per unit length. The manipulator and gripper also introduce inertial terms to the quadrotor dyad shown above. For simplification of the analysis we can take the pose of the gripper to be fully extended. This will produce the largest acting moment on the quadrotor body. The distance to the centre of mass can be calculated as $r_{com} = \sum r_i m_i / \sum m_i$ where indices i indicate the modeled point masses consisting of links a_0, a_1 and a_2 the arm motor masses m_1 and m_2 and lastly the mass of the gripper, m_g. Here r and m represent the distance to the modelled bodies and their individual masses, respectively (Figure 3).

After calculating the position of the center of mass with respect to the origin of the body frame we use the parallel axis theorem to calculate the inertial effect the manipulator arm has about the quadrotor origin. This can be expressed as:

$$I_{manip} = diag(m_{total}(r_{x'}\cos\theta)^2, m_{total}(r_{x'}\sin\theta)^2, m_{total}r_z^2. \quad (4)$$

This inertia can be summed with the inertia tensor of the quadrotor to express the total inertia with the manipulator and gripper attached. The design objective of the mechanical system level optimization is thus to minimize the net inertia of the system. To develop an objective function that achieves this goal, we take the trace of the overall inertia. It is suitable for the cost objective because it is invariant under similarity transformations and thus is a consistent metric regardless of device orientation. The system-level gripper optimization problem was altered to consist of a mass minimization problem, and we take the number of graspable objects to be a lower bound box constraint. The mass and the number of graspable objects is a direct tradeoff; as such, a detailed study of the N_{min} parameter, which denotes the minimum number of allowable graspable objects, is necessary. The negative null form for the optimization process can then be expressed as Equation (5), while the design variables and parameters are described in Table 1 and Figure 3 respectively. The mechanical system is optimized with respect to this objective. Following the mechanical system optimization, the net inertia and overall mass are calculated using the output design variables and then passed to the control optimization subsystem to calculate the required gains to minimize the l_2 norm of the system associated with kinetic energy.

$$\min_{x;p} J_{total} = 8m_{act}L_a^2 + \frac{2L_a^3\kappa}{3} + m_{total}[(r_{x'}cos\theta)^2 + (r_{x'}sin\theta)^2 + r_z^2] \quad (5)$$

$$x = \left[D_p, n_p, C_{bat}, W_m, a_0, a_1, a_2, l_a, l_p, l_d, t_p, t_d\right], \quad (6)$$

$$p = \left[V_{bat}, \kappa, r_{i0}, r_{o0}, r_{i1}, r_{o1}, r_{i2}, r_{o2}, \rho, \sigma_{yld}, m_1, m_2, \tau_1, \tau_2, \rho_g, \beta, h_g, \sigma_g, SF, f_c, \alpha, d_a, d_p, d_d, N_{min}\right]. \quad (7)$$

Subject to:

$$g_1(x;p) = 0.2h - FT \le 0, \qquad g_9(x;p) = \sigma_{2,bend}^{max} - 0.5\sigma_{yld} \le 0,$$

$$g_2(x;p) = 4 - PC \le 0, \qquad g_{10}(x;p) = M_1 - \tau_{mot} \le 0,$$

$$g_3(x;p) = I_{tot} - 0.03 \le 0, \qquad g_{11}(x;p) = M_2 - \tau_{mot} \le 0,$$

$$g_4(x;p) = 0.2s - \tau \le 0, \qquad g_{12} = \tau\left(l_p - d_p\right)\sin\gamma + 0.25\tau l_p \sin\beta - a_y l_p - 0.5 f_c l_p = 0,$$

$$g_5(x;p) = -V + V_{min} \le 0, \qquad g_{13}(x;p) = |(0.5l_d - d_d)f_c| - \left(\frac{1}{6}\sigma t_d^2 w\right) - \left(\frac{1}{6}SF\right)\sigma_g t_d^2 h_g \le 0,$$

$$g_6(x;p) = a_2/a_1 - 1.15 \le 0, \qquad g_{14}(x;p) = \left|a_y d_p\right| - \left(\frac{1}{6}SF\right)\sigma_g\left(t_p + d_p\tan\alpha\right)^2 h_g \le 0,$$

$$g_7(x;p) = \sigma_{0,bend}^{max} - 0.5\sigma_{yld} \le 0, \qquad g_{15} = \left|a_y d_p + 0.25 f_c l_p\right| - \left(\frac{1}{6}SF\right)\sigma_g\left(t_p + 0.75 l_p\tan\alpha\right)^2 h_g \le 0,$$

$$g_8(x;p) = \sigma_{1,bend}^{max} - 0.5\sigma_{yld} \le 0, \qquad g_{16}(x;p) = N_{min} - N \le 0,$$

(8)

Table 1. Optimization Problem Nomenclatures

Symbol	Description (Unit)	Symbol	Description
FT	Flight time (sec)	PC	Payload capacity (Kg)
I_{tot}	Total inertia (Kg. m^2)	τ	Motor time constant
D_p	Propeller diameter (m)	κ	Rotor arm unit mass (Kg/m)
n_p	Propeller angular veloc. (rev/s)	W_m	Rotors motor power (W)
C_{bat}	Battery capacity (Ah)	V_{bat}	Battery voltage (V)
m_1, m_2	Arm motor masses (Kg)	a_i	Manipulator D-H parameters (m)
τ_1, τ_2	Arm motor torques (N.m)	r_{i0}, r_{i1}, r_{i2}	Manipulator's links inner radii(m)
ρ	Manipulator links density (kg/m)	r_{o0}, r_{o1}, r_{o2}	Manipulator's links outer radii(m)
ρ_g	Gripper links density (kg/m)	σ_{yield}	links yield stress (Pa)
l_a, l_p, l_d	Gripper lengths (m)	α	Grip. distal link taper angle (deg)
t_p, t_d	Gripper thickness values (m)	β	Gripper's lower proximal tendon routing angle
σ_g	Gripper max flexural Stress (Pa)	d_a	Gripper's lower proximal tendon routing pt. (m)
SF	flexural Stress safety factor	d_p	Gripper's upper proximal tendon routing pt. (m)
f_c	Gripper's contact force (N)	d_d	Gripper's distal link routing point (m)
N_{min}	Min. number of graspable objects	h_g	Finger width (m)

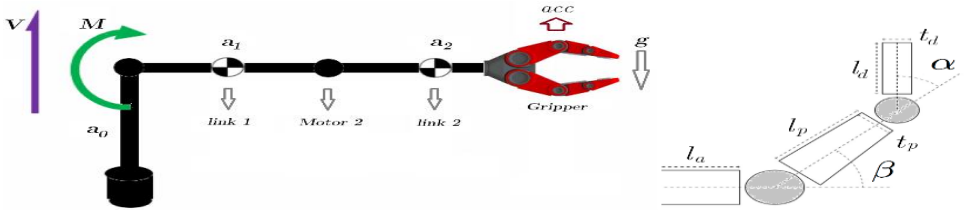

Figure 3. Schematic representations of the 3R elbow manipulator arm and attached gripper

4.2 Design Space Exploration

To better understand the behaviour of the objective function with respect to each design variable, the full design space was sampled using the Latin Hypercube method (McKay et al., 1979) . The objective function was evaluated at the sampled points and its value was plotted against each design variable individually in Figure 4. The trends highlighted by the design space exploration gave further insight into the design problem. Given the total device inertia as the objective function, the first manipulator link length, a_0, and the gripper proximal thickness, t_p, both greatly increases the device inertia as they increase (among feasible designs). Intuitively these both make sense as either increasing the mass or the length the device's extremities will incur a larger device inertia. Moreover, any increases in gripper mass have a substantial effect on the manipulator geometry, due to inertial effects.

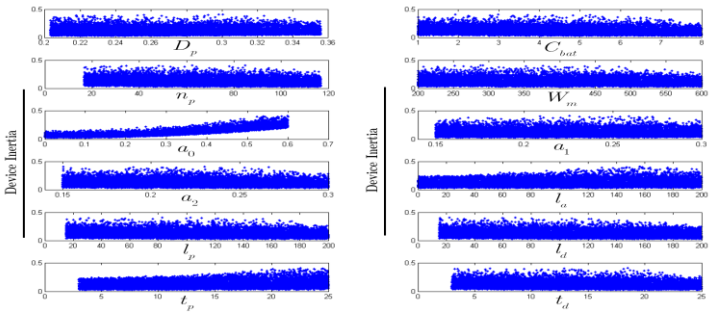

Figure 4. Exploration of design space using the Latin Hypercube method

4.3 Solutions and Results

The mechanical system optimization was conducted using the Sequential Quadratic Programming (SQP) method and the *fmincon* function of MATLAB Optimization Toolbox. A number of optimizations runs were carried out with various initial guesses and a number of local minima were found. However, the process was sensitive to local minima. As such, numerous random restarts were necessary to achieve a result closer to global minimum. Once the optimization was completed for the mechanical system the results of the device were passed to the integrated mechanical-control system optimization stage. The key inputs were the total device inertia that was the objective of the mechanical integration and rotor arm lengths. The results are displayed in Table 2.

5 INTEGRATED MECHANICAL-CONTROL SYSTEM OPTIMIZATION

5.1 Algorithm

In order to perform an efficient system integration for the proposed quadrotor UAV system, an iterative process has been considered for the overall mechanical-control system optimization. This process is described in Figure 5. After performing the mechanical system optimization, the first generation of structural parameters, i.e. Inertia tensor and accordingly mass and arm lengths are produced (Figure 6). Passing these parameters to the control system and by solving an optimization problem to find the best settling time subjected to various control performance constraints, twelve PID gains for Roll, Pitch, Yaw angles and altitude, , are generated. For this process, the overall objective function is defined as:

$$f(x;p) = t_s = \alpha_\phi t_{s,\phi} + \alpha_\theta t_{s,\theta} + \alpha_\psi t_{s,\psi} + \alpha_z t_{s,z}, \tag{9}$$

$$x = \text{PID Gains}, \quad p = [m, g, l, I_{xx}, I_{yy}, I_{zz}, J_r, \Omega_i, T_i], \tag{10}$$

which aggregates the settling time values from altitude and attitude control systems. These values can be calculated algorithmically as the time required for the response curve to reach and stay within a range of certain percentage (usually 5% or 2%) of the final value. In Eq. 10, m is the system's total mass, I is the inertia tensor, J_r is the rotor inertia, Ω_i is rotors speeds and T_i is induced torque by each rotor.

Table 2. Mechanical system optimization results

Algorithm	Matlab Optimization Toolbox: fmincon; sqp
Termination Criteria	Iterations: 1000, Function Evaluations: 3000, Step Tolerance: 1E-4
Termination Results	Iterations: 14, Function Evaluations: 286, Step: 7.16E-5
Initial Guess	$x_0 = [D_p, C_{bat}, n_p, W_m, a_0, a_1, a_2, l_a, l_p, l_d, t_p, t_d]$ $x_0 = [0.24, 3, 92.4, 501.5, 0.152, 0.157, 0.1, 10.8, 113.2, 159.15, 23.5, 5.9]$
Possible Local Optima	$x^* = [0.32, 8, 79.4, 530.2, 0.31, 0.15, 0.15, 0, 75.3, 63.3, 10.6, 7.16]$ $f^* = 0.0772$
Active Constraints	lambda.eqnonlin = [0.7059] lambda.lower = [0 0 0 0 0 307.58 284.18 0 0 0 0 0] lambda.upper = [100 0 94.5 100 100 0 0 100 100 0 0 100 100] lambda.ineqnonlin=[0 5.4 0 0 0 0 0 0 0 0 0 2.5 0.08 0 0 0]

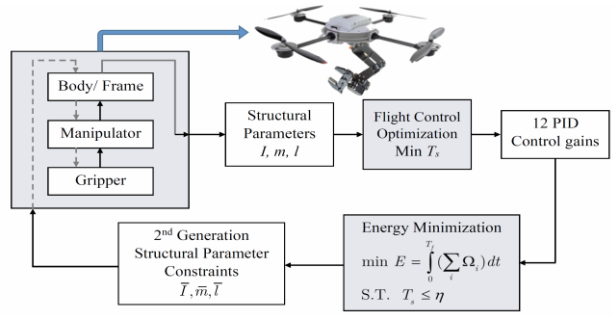

Figure 5. The process of system-level optimization for integrated design of a quadrotor UAV

name	parameter	value	unit [mksA]
mass	m	1.374	kg
inertia on x axis	I_{xx}	0.05109	kg.m^2
inertia on y axis	I_{yy}	0.05109	kg.m^2
inertia on z axis	I_{zz}	0.02162	kg.m^2
thrust coefficient	b	3.13e-5	N s^2
drag coefficient	d	7.5e-7	Nm s^2
propeller radius	R_{rad}	0.15	m
propeller chord	c	0.04	m
pitch of incidence	θ_0	0.26	rad
twist pitch	θ_{tw}	0.045	rad
rotor inertia	J_r	6e-5	kg.m^2
arm length	l	0.229	m

Figure 6. First generation of the structural parameters

The closed-loop transfer functions for attitude flight control system based on which the step response properties are calculated are:

$$T_{tb}(s) = \frac{\Gamma_{tb}(k_{d,tb}s^2 + k_{p,tb}s + k_{i,tb})}{s^3 + \Gamma_{tb}(k_{d,tb}s^2 + k_{p,tb}s + k_{i,tb})}, \tag{11}$$

where tb is the Tait-Bryan angles as $tb = [\phi, \theta, \psi]$, and $\Gamma_\Phi = \frac{l}{I_{xx}}$, $\Gamma_\Phi = \frac{l}{I_{yy}}$, $\Gamma_\Phi = \frac{1}{I_{zz}}$, while $a_o = (9.81 - 3.5/m), a_1 = 3.49, a_2 = 0.304, a_3 = 0.356$ and $a_4 = 0.0315$. Now, the corresponding step-response properties such as rise-time, maximum overshoot, phase and gain margins, cut frequency and pick-time can be also formulated algorithmically and considered as the control system design criteria i.e. constraint functions as detailed in Equation 12.

$$\begin{aligned} &g_{1-4} = MP - 15\% \leq 0, \\ &g_{5-8} = -MP + 15\% \leq 0, \end{aligned} \quad \begin{aligned} &g_{9-12} = t_r - 1sec \leq 0, \\ &g_{13-16} = -GM + 6dB \leq 0, \end{aligned} \quad \begin{aligned} &g_{17-20} = -PM + 70deg \leq 0. \end{aligned} \tag{12}$$

The whole process is also subjected to stability conditions and variable bounds. Solving this optimization problem provides us with 12 initial optimal PID gains. According to Figure 5, considering these initial optimal gains as constant parameters, another control system optimization process can be defined to solve for the structural variable, that minimizes the consumed energy by four propeller actuators. In our simulations, the time integral of all four motor speeds is proportional to the total energy used. Calculation of the actual energy used by the UAV in traversing a flight path would require a precise model for the motor. This seems unnecessary for our purpose since the time integral of the motor speeds and the total energy used will have the same effective minimum. Since the control input is calculated as part of the control algorithm anyway, it is used as a performance metric. The new system-level optimization process can be formulated as follows:

$$\min_x f(x;p) = E_r(x;p) = \int_0^{T_f} (\sum_i \Omega_i) dt \tag{13}$$

$$x = [x_1, x_2, x_3, x_4, x_5, x_6] = \left[m, g, l, I_{xx}, I_{yy}, I_{zz}, J_r, \Omega_i, T_i\right], \quad p = \text{PID Gains.} \tag{14}$$

New design constraints can be also listed as follows; (: Group of constraints)

$$\begin{aligned} &G_1 = MP - 15\% \leq 0, \\ &G_2 = -MP + 5\% \leq 0, \\ &G_3 = t_s - \eta \leq 0, \end{aligned} \quad \begin{aligned} &G_4 = t_r - 1sec \leq 0, \\ &G_5 = -GM + 6dB \leq 0, \\ &G_6 = -PM + 50\ deg \leq 0, \end{aligned} \quad \begin{aligned} &G_7 = Routh - Hurwitz\ Stability \leq 0, \end{aligned} \tag{15}$$

5.2 Optimization Results

After implementing the objective function and constraints using MATLAB scripts, the *fmincon* function has been used along with the SQP algorithm to solve the optimization problem based on 3 initial guesses. Moreover, to ensure the global minimum, a Multi-Start algorithm has been used. Table 3 shows a set of

analytical results known as second generation structural parameters. The new solutions are passed to the mechanical system as new initial guesses and variable bounds, through a number of iterations and at the end, a final optimal system with regards to control performance and consumed energy will be achieved. Figure 7 numerically describes a brief process for two iterations, while Figure 8 shows the control system performance based on the new structural parameters and PID gains.

Table 3. Results for the minimization of the consumed energy

	Run 1	Run 2	Run 3	MultiStart
x_0	[1.3, 0.23, 0.055, 0.055, 0.022, 6e-5]	[1, 0.20, 0.050, 0.050, 0.030, 6e-5]	[0.9, 0.22, 0.051, 0.051, 0.020, 6e-5]	-
# of Iter.	37	19	22	133
x^*	[1.29, 0.23, 0.0448, 0.0448, 0.029, 6e-5]	[1.182, 0.224, 0.0389, 0.0389, 0.0192, 6e-5]	[0.832, 0.188, 0.0511, 0.0511, 0.0296, 6e-5]	[1.182, 0.224, 0.0389, 0.0389, 0.0192, 6e-5]
f^*	1.18e+5	9.6431e+4	1.2562e+5	9.6431e+4
Max g^*	8.3011e-008	9.1778e-007	7.7135e-008	9.1778e-007
# of Active Constraints	19	17	19	17

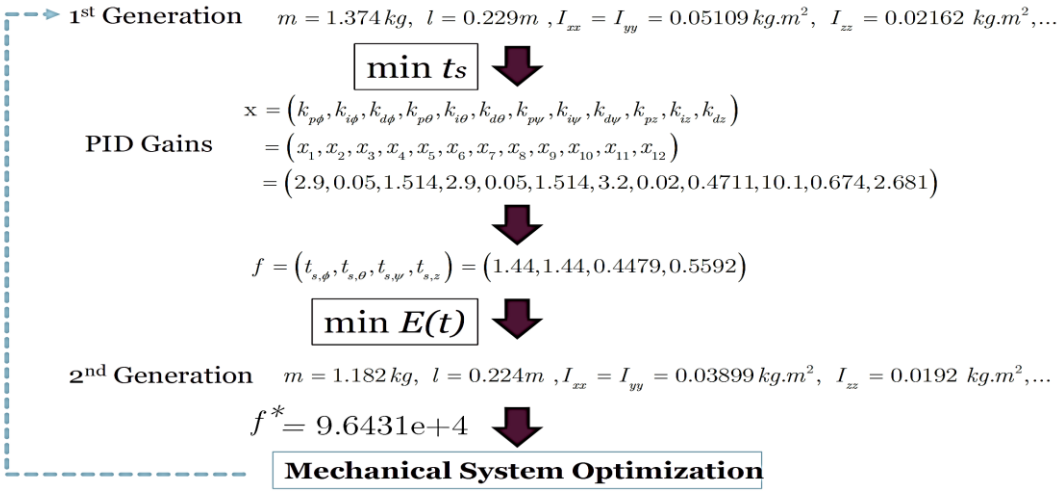

Figure 7. Mechanical-Control System optimization process and results for two iterations

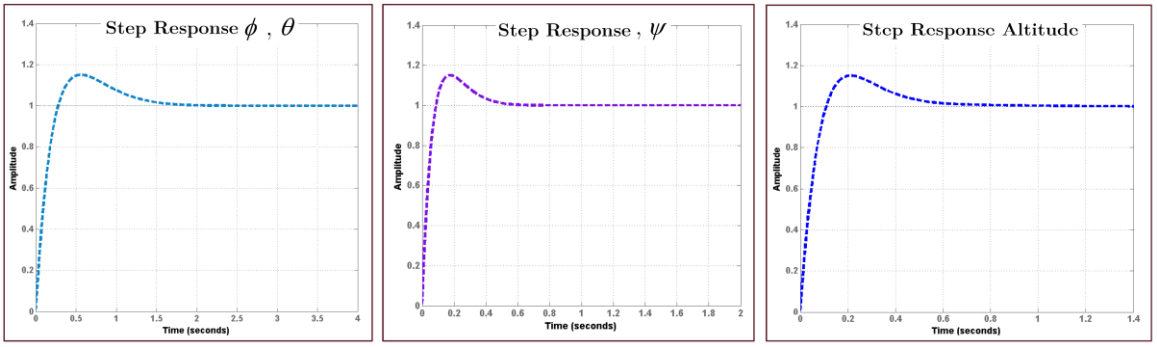

Figure 8. The step-response of the attitude and altitude control systems

6 CONCLUSION AND DISCUSSION

The mechanical system optimization differed greatly from the results at the sub-system level, the change in objective and increase in constraints created a much more complicated problem. The design trade-offs that were more apparent in the sub-system optimization were much more difficult to identify. The results of the mechanical optimization reflected a much more compact but also more powerful design of the quadrotor than when compared to the sub-system optimization. It has much larger battery and much more powerful motors but also a smaller rotor arm length. Through the system level optimization, the gripper also resulted in a much more compact design. The gripper geometry remained largely the same due to the constraint on the number of graspable objects remaining the same, but the palm length was driven to zero. The geometry of the gripper only varied in the distal link length, which was largely governed by the stress constraints in the gripper. Due to the interaction of constraints, as well as the added constraints that were previously governed by the subsystem-level objective functions, the feasible design space is far smaller than what it previously was. Additionally, the number of variables for each subsystem was decreased to reduce the complexity of the full optimization. In addition to the number of design variables decreasing, the constraints from the subsystems were mostly retained. The result of these changes is that the feasible design space is far smaller than the feasible spaces for each component.

REFERENCES

Bouabdallah, S. and R. Siegwart (2007), Full control of a quadrotor. Intelligent robots and systems, 2007. IROS 2007. IEEE/RSJ international conference on, IEEE.

Chu, P. and H. Duan (2013), Quadrotor flight control parameters optimization based on chaotic estimation of distribution algorithm. Advances in Neural Networks–ISNN 2013, Springer: 19-26.

Ciocarlie, M., F. M. Hicks, R. Holmberg, J. Hawke, M. Schlicht, J. Gee, S. Stanford and R. Bahadur (2014), "The Velo gripper: A versatile single-actuator design for enveloping, parallel and fingertip grasps." The International Journal of Robotics Research 33(5): 753-767.

Garage, W. (2010), The household objects SQL Database, June.

Hoffmann, G. M., H. Huang, S. L. Waslander and C. J. Tomlin (2007), Quadrotor helicopter flight dynamics and control: Theory and experiment. Proc. of the AIAA Guidance, Navigation, and Control Conference.

Magnussen, O., G. Hovland and M. Ottestad (2014), Multicopter UAV design optimization. Mechatronic and Embedded Systems and Applications (MESA), 2014 IEEE/ASME 10th International Conference on, IEEE.

McKay, M. D., R. J. Beckman and W. J. Conover (1979), "A Comparison of Three Methods for Selecting Values of Input Variables in the Analysis of Output From a Computer Code." Technometrics 42(1): 55-61.

Mohebbi, A., S. Achiche and L. Baron (2015), Integrated Design of A Vision-Guided Quadrotor UAV: A Mechatronics Approach. 2015 CCToMM Symposium on Mechanisms, Machines, and Mechatronics, Canadian Committee for the Theory of Machines and Mechanisms.

Mohebbi, A., S. Achiche and L. Baron (2016), "Design of a Vision Guided Mechatronic Quadrotor System Using Design For Control Methodology." Transactions of the Canadian Society for Mechanical Engineering 40(2): 201-219.

Salih, A. L., M. Moghavvemi, H. A. Mohamed and K. S. Gaeid (2010), Modelling and PID controller design for a quadrotor unmanned air vehicle. Automation Quality and Testing Robotics (AQTR), 2010 IEEE International Conference on, IEEE.

Sobieszczanski-Sobieski, J. and R. T. Haftka (1997), "Multidisciplinary aerospace design optimization: survey of recent developments." Structural optimization 14(1): 1-23.

Szafranski, G. and R. Czyba (2011), Different approaches of PID control UAV type Quadrotor. International Micro Air Vehicle conference and competitions 2011 (IMAV 2011),'t Harde, The Netherlands, September 12-15, 2011, Delft University of Technology and Thales.

Turkoglu, K., U. Ozdemir, M. Nikbay and E. M. Jafarov (2008), "PID parameter optimization of an UAV longitudinal flight control system." Engineering and Technology 35.

Yacef, F., O. Bouhali, M. Hamerlain and A. Rezoug (2013), PSO optimization of Integral backstepping controller for quadrotor attitude stabilization. Systems and Control (ICSC), 2013 3rd International Conference on, IEEE.

Yoshikawa, T. (1985), Dynamic manipulability of robot manipulators. Robotics and Automation. Proceedings. 1985 IEEE International Conference on, IEEE.